

PREPARED FOR THE U.S. DEPARTMENT OF ENERGY,  
UNDER CONTRACT DE-AC02-76CH03073

PPPL-3717  
UC-70

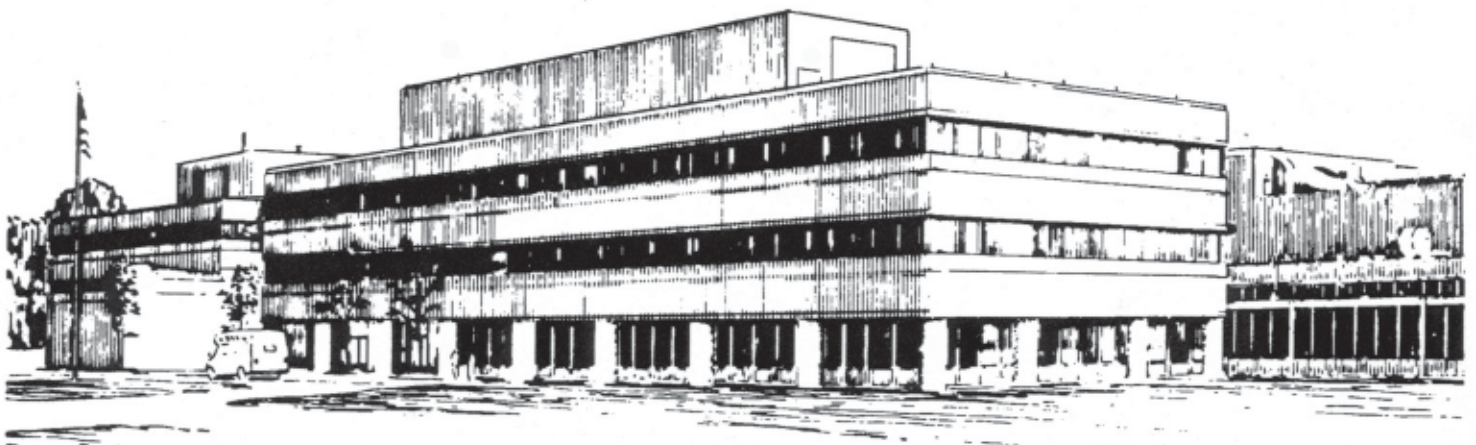
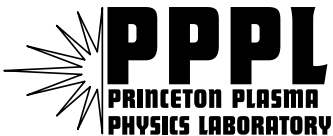
PPPL-3717

**Study of Thermonuclear Alfvén Instabilities  
in Next Step Burning Plasma Experiments**

by

N.N. Gorelenkov, H.L. Berk, R. Budny, C.Z. Cheng, G.-Y. Fu,  
W.W. Heidbrink, G. Kramer, D. Meade, and R. Nazikian

July 2002



**PRINCETON PLASMA PHYSICS LABORATORY  
PRINCETON UNIVERSITY, PRINCETON, NEW JERSEY**

## **PPPL Reports Disclaimer**

This report was prepared as an account of work sponsored by an agency of the United States Government. Neither the United States Government nor any agency thereof, nor any of their employees, makes any warranty, express or implied, or assumes any legal liability or responsibility for the accuracy, completeness, or usefulness of any information, apparatus, product, or process disclosed, or represents that its use would not infringe privately owned rights. Reference herein to any specific commercial product, process, or service by trade name, trademark, manufacturer, or otherwise, does not necessarily constitute or imply its endorsement, recommendation, or favoring by the United States Government or any agency thereof. The views and opinions of authors expressed herein do not necessarily state or reflect those of the United States Government or any agency thereof.

## **Availability**

This report is posted on the U.S. Department of Energy's Princeton Plasma Physics Laboratory Publications and Reports web site in Fiscal Year 2002. The home page for PPPL Reports and Publications is: [http://www.pppl.gov/pub\\_report/](http://www.pppl.gov/pub_report/)

DOE and DOE Contractors can obtain copies of this report from:

U.S. Department of Energy  
Office of Scientific and Technical Information  
DOE Technical Information Services (DTIS)  
P.O. Box 62  
Oak Ridge, TN 37831  
  
Telephone: (865) 576-8401  
Fax: (865) 576-5728  
Email: [reports@adonis.osti.gov](mailto:reports@adonis.osti.gov)

This report is available to the general public from:

National Technical Information Service  
U.S. Department of Commerce  
5285 Port Royal Road  
Springfield, VA 22161  
  
Telephone: 1-800-553-6847 or  
(703) 605-6000  
Fax: (703) 321-8547  
Internet: <http://www.ntis.gov/ordering.htm>

# Study of Thermonuclear Alfvén Instabilities in Next Step Burning Plasma Experiments.

N. N. Gorelenkov<sup>†</sup>, H. L. Berk<sup>‡</sup>, R. Budny<sup>†</sup>, C. Z. Cheng<sup>†</sup>, G.-Y. Fu<sup>†</sup>  
W.W. Heidbrink<sup>♭</sup>, G. Kramer<sup>†</sup>, D. Meade<sup>†</sup>, R. Nazikian<sup>†</sup>

<sup>†</sup>*Princeton Plasma Physics Laboratory*

*P.O. Box 451, Princeton, NJ 08543-0451.*

<sup>‡</sup>*IFS, Austin, Texas.*

<sup>♭</sup>*University of California, Irvine, California 92697.*

This work supported by DoE contract No. DE-AC02-76-CHO-3073.

## ABSTRACT

A study is presented for the stability of  $\alpha$ -particle driven shear Alfvén Eigenmodes (AE) for the nominal parameters of the three major burning plasma proposals, ITER, FIRE and IGNITOR. A study of the JET plasma, where fusion alphas were generated in tritium experiments, is also included to attempt experimental validation of the numerical predictions. An analytic assessment of Toroidal AE (TAE) stability is first presented, where the alpha particle beta due to the fusion reaction rate and electron drag is simply and accurately estimated in  $7 - 20\text{keV}$  plasma temperature regime. In this assessment the hot particle drive is balanced against ion-Landau damping of the background deuterons and electron collision effects and stability boundaries are determined. Then two numerical studies of AE instability is presented. In one the High-n stability code HINST is used. This code is capable of predicting instabilities of low and moderately high frequency Alfvén modes. HINST computes the non-perturbative solutions of the Alfvén eigenmodes including effects of ion finite Larmor radius, orbit width, trapped electrons etc.. The stability calculations are repeated using the global code NOVAK. We show that for these tokamaks the spectrum of the least stable AE modes are TAE that appear at medium-/high-n numbers. In HINST

TAEs are locally unstable due to the alphas pressure gradient in all the devices under the consideration except IGNITOR. However, NOVAK calculations show that the global mode structure enhances the damping mechanisms and produces stability in all configurations considered here. A serious question remains whether the perturbation theory used in NOVAK overestimates the stability predictions, so that it is premature to conclude that the nominal operation of all three proposals are stable to AEs. In addition NBI ions produce a strong stabilizing effect for JET. However in ITER the beam energies needed to penetrate to the core must be high so that a diamagnetic drift frequency comparable to that of the alpha particles is produced by the beam ions which induces a destabilizing effect.

## I. INTRODUCTION

In a fusion producing deuterium-tritium (D-T) tokamak plasma it is intended that the  $3.5MeV$  alpha particles be trapped by the magnetic field and their energy be then transferred, primarily through electron drag, to the background plasma. It is the purpose of a burning plasma (BP) experiment to demonstrate that this method of self-heating will be the dominant method of heating of a plasma that is producing fusion energy. However, the alpha particle partial pressure is significant and a physical issue arises whether this pressure is capable of inducing collective behavior that may cause the premature loss of alpha particles. Should this be the case, two major problems may arise: (i) it may become difficult to sustain the plasma parameters close to the ignition and (ii) the alpha fluxes of energetic alpha particles ( $\sim 3.5MeV$ ) to the first wall of the experiment can cause severe wall damage.

Indeed it has been demonstrated in present day (PD) experiments that the collective effects induced from energetic particles can result in premature alpha particle loss. However, it is difficult to obtain a comprehensive extrapolation of the results of PD experiments to what would be expected for BP experiments. The distribution functions are often quite different. In PD experiments the energetic particle distribution are anisotropic whereas in a BP experiment the distribution function of fusion alpha particles is isotropic. In addition

in a BP experiment the machine size to orbit width will be significantly larger and the spectrum (and number) of unstable modes is likely to be broader in BP compared with PD experiments. Thus even with continued study in PD experiments, extrapolation to reliable predictions for BP experiments may remain uncertain without actually performing these BP experiments.

It is now generally believed that the Toroidal Alfvén Eigenmodes (TAE) [1–4] destabilized by fast ions, are the plasma waves most likely to cause significant difficulties for the containment of energetic alpha particles in fusion energy generating tokamak experiments. It has already been experimentally established that in presence of a strong enough energetic particle energy density that these mode will induce large losses of fast particles, though it is also known that there is a wide variety of conditions where these modes are stable or when unstable, do not induce anomalous loss. Experimental reviews of TAE and other relevant issues of fast particle physics can be found in Ref.[5, 6]. It is the purpose of this paper to determine whether linear instability to the TAE mode is to be expected under burning plasma conditions. In particular we study TAE stability for the three proposed BP experiments now being considered by the fusion research community, ITER-FEAT, FIRE and IGNITOR. By in large we will numerically study the stability for the proposed nominal operating conditions. However, with use of analytic estimates some extrapolation is possible to other temperature regimes of operation.

We will present three types of stability analyses here. The first is based on a simplified analytic analysis where we use an estimate for the alpha particle drive and compare it to two damping mechanisms that are expected to dominate for most the parameters relevant to the machines being proposed and their modes of excitation. The analytic study is based on simplified scaling, under the assumption that the base TAE structure of "couplet" formed at  $q(r) = (m + 1/2)/n$  by two poloidal mode numbers with values  $m$  and  $m + 1$ , can be used to characterize the stability of the global mode structure even though a realistic mode structure is generally more complex than the assumed local structure. We will see that this analysis correlates favorably with detailed numerical calculations. Therefore the analytic

analysis gives a guide as to how stability conditions change as parameters of the proposed experiment are varied from the nominal machine parameters that the numerical studies concentrate upon.

The second method is the numerically study the problem with the recently develop HINST code (high- $n$  toroidal stability) [7], which has been recently improved to describe the effect of finite orbit width as well as the finite Larmor radius of the energetic particles in realistic numerical equilibrium. HINST is a high- $n$  ballooning code that can be applied accurately to even moderate  $n$ - numbers (e.g.  $n \sim 5$ ). It is limited by being a localized code, and as such does not account for the extended spatial mode structure of a TAE mode. However, HINST has the virtue of being a non-perturbative code. As such it can describe the so-called Resonant TAE (RTAE)[8] [alternatively called the Energetic Particle Mode (EPM)[9–11]] energetic particle modes that can even arise in MHD continuum. Such modes may be related to experimentally observed Beta-Induced Alfvén Eigenmodes (BAE) [12, 13]. Further, an extremely important damping mechanism, radiation damping, is precisely treated in HINST. Previously in full machine codes that made extensive studies of TAE instability in realistic designed experiments (such as NOVA) radiation damping was only treated perturbatively, which apparently under-estimates the damping. Other codes, such as CASTOR-K [14] treat radiation damping in a non-perturbative manner, but the instability drive is still treated perturbatively. It should be noted that radiation damping becomes a particularly dominant damping mechanism when the radiative damping rate of TAE due to core ion finite Larmor radius (FLR) effects increases with increasing  $k_{\perp}\rho_i$  [8, 15] and becomes strongly stabilizing effect at  $k_{\perp}\rho_i \sim \sqrt{r/R}$ , where  $k_{\perp}$  is the characteristic radial wavenumber of a TAE mode and  $\rho_i$  is the bulk ion Larmor radius calculated for ions with thermal velocity  $v_T = \sqrt{2T/m}$ . This damping mechanism may then compete with the alpha particle drive at moderately high toroidal mode number  $n$ . The fast particle drive reaches a maximum for  $n$ -numbers near  $nq^2\rho_h/r \simeq 1$ , where  $\rho_h$  is the fast ion Larmor radius, and then beyond this value decreases with increasing  $n$ . Depending on detailed parameters, radiation damping may be a significant damping mechanisms near the peak of the alpha particle drive. In addition

HINST includes in a non-perturbative manner, damping from ion Landau damping, electron collisionality, and electron Landau damping.

The third stability study of the proposed nominal parameters of the BP experiments comes using the NOVA-K code. This is basically the same code that was used to study the TAE stability of the original ITER design. This code is a perturbative code, that obtains an extended mode structure by neglecting damping and drive sources, and then incorporating these sources through a perturbative procedure. This code has the virtue of being a full machine code, and if there is no difficulty of exciting the continuum at some radial position, the global structure of the TAE mode is determined. The alpha particle drives and the numerous damping mechanisms (including a model for radiation damping) is then incorporated in a perturbative manner to predict stability.

It should be noted that there are deficiencies in the procedure used in the NOVA code. Frequently, the continuum cannot be avoided and the damping, as well as alteration of mode structure due to the presence of the continuum, is ignored. At higher  $n$ -values that are studied in this code, there is a tendency for the TAE modes at a given  $n$ -number to be nearly degenerate. This give rise to the possibility that the basic mode structures may be different than the zeroth order structures (which often extend through a large fraction of the plasma) that emerge from the code. Of particular concern is the tendency for strong collisional damping arising from the mode structure at the outer edge of the plasma, to stabilize a mode where the drive is located in the central region of the plasma. A more sophisticated perturbation theory may need to be implemented to determine if TAE modes might to localize to regions where the drive dominates. However, for this study we report solely on the predictions of the present code with its present calculational method.

## II. ANALYTICAL STABILITY MODEL

### A. Fast particle TAE drive.

To understand the parametric dependence of the drive of TAE modes we use the model that the alpha particles are created at  $\mathcal{E}_{\alpha 0} = 3.52 \text{ MeV}$  and then slow down due to electron drag. It is adequate to take the alpha particle distribution function of the form,  $f_0(v) \simeq 2^{-5} 3\pi^{-2} \beta_\alpha B^2 \theta(v_{\alpha 0} - v) / (\mathcal{E}_{\alpha 0} v^3)$ , with  $\beta_\alpha$  the alpha particle beta value,  $\theta(x)$  a step function,  $v_{\alpha 0}$  the birth speed of an alpha particle.

The alpha particle drive,  $\gamma_\alpha / \omega$ , will be in a plateau regime [17, 18, 22] for the dependence on  $n$ -values of the toroidal mode lying in the regime

$$n_{min} \simeq \frac{r}{R} n_{max} < n < n_{max} \simeq \frac{r \omega_{c\alpha}}{q^2 v_A}. \quad (1)$$

The appropriate expression for the growth rate in this plateau regime was obtained in Refs.[17, 18]. Comparison of this analytic expression with the numerical calculations in NOVA-K in the limit of a low beta when the flux surface is spherical shows quantitative agreement when FLR effects are neglected. The growth rate when the shear  $s$  is less than unity (with the factor insensitive to  $s$  as it approaches unity) is found to be,

$$\frac{\gamma_\alpha}{\omega} \simeq -\frac{5\pi}{2} q^2 r \frac{\partial \beta_\alpha}{\partial r} x_A (1 - x_A^2), \quad (2)$$

where  $x_A = v_A / v_{\alpha 0} < 1$  and in ref [22] the effect of FLR is found to lower this plateau result by about 20% for core localized TAEs.

### B. Damping mechanisms

The damping rate dependence on plasma parameters is more complicated and includes TAE energy radiation through the thermal ion FLR effects (as well as comparable electron impedance effects) which leads to a modification of the eigenfunction. Different contributions

to damping can be expressed analytically in a limited domain of plasma parameters and are incorporated later in the NOVAK study. Radiation damping expression from Refs.[16, 21] is very sensitive to plasma parameters, and is difficult to incorporate into a simple expression that is a typical value for the entire machine. However, frequently radiation damping is negligible and a reasonable estimate of the damping can be obtained by only including the thermal ion Landau damping from deuterons and trapped electron collisional damping, as we will see below in Sec.III A. The analytic formula for Landau damping of Maxwellian ions [4], which is applicable to the large aspect ratio localized TAE solutions, is:

$$\frac{\gamma_{iLand}}{\omega} = -\frac{q^2 \sigma \sqrt{\pi} \beta_{pc}}{2(1+\sigma)} x_i^5 e^{-x_i^2} = -\frac{q^2 \sigma \sqrt{\pi}}{18(1+\sigma/4)} x_i^3 e^{-x_i^2} \quad (3)$$

where  $\sigma = (n_D + n_T) / n_e$  is the plasma ion depletion factor close to unity,

$$x_i = v_A / 3v_i \simeq \sqrt{(1+\sigma) / 9(1+\sigma/4)} \beta_{pc}, \quad (4)$$

$\beta_{pc}$  is the core plasma beta which includes thermal electrons and ions,  $v_i = \sqrt{2T_i/m_i}$  is the ion thermal velocity.

Here we assumed  $x_i \gg 1$ , so that in a deuterium-tritium plasma mixture only deuterium contributes to the damping rate, since its thermal velocity is larger than the tritium one. Note, that in Ref.[22] this formula was shown to accurately describe ion Landau damping for core localized TAEs. For simplicity we assume that there is only one impurity specie with mass to charge ratio the same as deuterium's.

The second major damping mechanism considered in this analytic study is the trapped electron collisional damping of TAE modes [23, 24], which becomes dominant in lower temperature/higher density plasmas. The damping can be approximately expressed as [24]

$$\frac{\gamma_e}{\omega} \simeq -\sqrt{\frac{\pi}{2}} \frac{1}{4} \left[ I_1 \left( \frac{8snq\rho_s}{5r\epsilon} \right)^2 + I_2 q^2 \frac{8\beta_{pc}}{1+\sigma} \right] \sqrt{\frac{\nu}{\omega}} \left[ \ln \left( 16\sqrt{\frac{\omega\epsilon}{\nu}} \right) \right]^{-3/2}, \quad (5)$$

where coefficients  $I_j$  with good accuracy can be approximated as follows  $I_1 = (0.43Z_{eff} + 1.06)$ , and  $I_2 = (1.03Z_{eff} + 2.3)$ . For one specie impurity we have  $Z_{eff} =$

$\sigma + Z_i(1 - \sigma)|_{Z_i=6} = 6 - 5\sigma$ . The electron collisional frequency is

$$\frac{\nu}{\omega} = \frac{4\pi n_e e^4 \ln(\Lambda_e)}{\omega m_e^2 v_e^3} \simeq \frac{2\sqrt{2}\pi}{3} \sqrt{\frac{m_p}{m_e}} \frac{n_e e^4 \ln(\Lambda_e) q R}{x_i T_e^2} \simeq 0.145 \frac{R_{[m]} q}{x_i^3} \frac{B_{[10T]}^2}{(1 + \sigma/4) T_{[10keV]}^3}, \quad (6)$$

where we assumed that electron Coulomb logarithm equals 20 and the plasma parameter subscripts in square brackets denotes the units to be used. The toroidal mode dependence in Eq.(5) suggests that for the most unstable mode we should take the lowest  $n$ -value that lies within the plateau regime of the alpha particle drive,  $n_{min}$ :

$$\frac{\gamma_e}{\omega} \simeq -\sqrt{\frac{\pi}{2}} \frac{1}{4} \left[ I_1 \left( \frac{4\sqrt{7}s}{15qx_i} \right)^2 \left( \frac{1}{\sigma} + \frac{1}{4} \right) + I_2 q^2 \frac{8}{9(1 + \sigma/4) x_i^2} \right] \sqrt{\frac{\nu}{\omega}} \left[ \ln \left( 16\sqrt{\frac{\omega\epsilon}{\nu}} \right) \right]^{-3/2}. \quad (7)$$

### C. Critical beta and stability boundary.

Comparing the drive, Eq.(2), and the damping, Eqs.(3,7) and noting that  $x_A = 0.226\sqrt{T_{[10keV]} x_i}$ , one can obtain the formula for the critical beta of hot particles:

$$\left( \frac{-\partial\beta_\alpha}{\partial \ln r} \right)_{cr} = \frac{0.156 T_{[10keV]}^{-1/2} x_i^{-1}}{1 - 0.051 T_{[10keV]} x_i^2} \left\{ \frac{\sigma x_i^3}{2\sqrt{2}} \frac{e^{-x_i^2}}{1 + \sigma/4} + \right. \\ \left. + x_i^{-2} \sqrt{\frac{\nu}{\omega \left[ \ln \left( 16\sqrt{\frac{\omega\epsilon}{\nu}} \right) \right]^3}} \left[ \frac{14}{25} \frac{I_1 s^2}{q^4} \left( \frac{1}{\sigma} + \frac{1}{4} \right) + \frac{I_2}{1 + \sigma/4} \right] \right\} \quad (8)$$

Note, that in Eq.(8) ion Landau damping term depends only on temperature and plasma beta.

It is useful to plot the stability diagrams in terms of device operating parameters. In order to accomplish this we express the alpha particle pressure gradient as a function of plasma beta and temperature:

$$\frac{\beta_\alpha}{\beta_{pc}} = \frac{8n_D n_T}{n_e^2 (1 + \sigma)} \frac{\langle \sigma v \rangle n_e \tau_{se} \mathcal{E}_{\alpha 0}}{12T} = \frac{\sigma^2}{1 + \sigma} 0.117 T_{[10keV]}^{5/2}, \quad (9)$$

where we approximated the fusion source as  $\langle \sigma v \rangle \simeq 10^{-16} T_{[10keV]}^2 cm^3/sec$ , which is accurate within  $0.7 < T_{[10keV]} < 2$ , and the energy slowing down time is  $n_e \tau_{se} = 2 \times 10^{13} T_{[10keV]}^{3/2} cm^{-3}s$ .

This formula gives the following estimate for the alpha particle pressure gradient:

$$\frac{-\partial\beta_\alpha}{\partial\ln r} \simeq \frac{7}{2}\beta_\alpha \frac{-\partial\ln T}{\partial\ln r} \simeq 0.0456 \frac{\sigma^2}{(1+\sigma/4)} x_i^2 T_{[10keV]}^{5/2} \frac{-\partial\ln T}{\partial\ln r}. \quad (10)$$

In present day experiments fast particle pressure gradient is determined by the deposition of the neutral beam or ICRH power.

Combining two equations, Eq.(8) and Eq.(10) results in an equation, that connects primarily three tokamak plasma parameters:  $\eta \equiv \frac{-\partial\ln T}{\partial\ln r}$ ,  $T$ , and  $\beta_{pc}$ . Analysis shows that if  $\epsilon$ ,  $q$ ,  $s$ ,  $\sigma$  are similar in the machines being considered, then the plasma parametric variation for different BPs comes primarily from the parameter  $RB^2$ , which happens to be nearly the same for all the BP proposals considered. If we assume that the temperature profiles parabolic  $T = T_0(1 - \Phi/\Phi_0)$ , where  $\Phi = (r/a)^2\Phi_0$  is the toroidal magnetic flux and  $\Phi_0$  is its value at the plasma edge, and  $r$  is the ‘‘averaged’’ minor radius of magnetic surface, we can express

$$T = \frac{T_0}{1 + \eta/2}, \quad \beta_{pc} = \frac{\beta_{pc0}}{1 + \eta/2}.$$

Note, that in this case averaged temperature is  $\langle T \rangle = 3T(\eta = 1)/4 = T_0/2$ .

In the assumption of the parabolic temperature profile and the fusion alpha beta determined by Eq.(10) one can show that since  $\eta \rightarrow \infty$  at the edge (and  $\frac{-\partial\beta_\alpha}{\partial\ln r} \rightarrow \infty$  and  $\gamma_\alpha \rightarrow \infty$ ), there is always such a minor radius above which TAEs are unstable. Figure 1 shows the critical magnetic surface minor radius  $(r/a)_{cr}$  above which the TAEs are unstable for different temperatures of the plasma ions  $T_0 = 20, 15, 12, 10keV$  and two different depletion factors for  $\sigma = 0.8$  and  $\sigma = 1$ . For depletion  $\sigma = 0.8$  TAEs are stable at  $T_0 = 10keV$ , which corresponds to IGNITOR parameters. However we should note, that our model is breaking down near the edge as alpha particle reaction rate, Eq.(9), is too large at  $T_i < 7keV$  and the collisional terms should take on a different form as well. In principle as we approach the edge stability will arise again but it is not seen in analytical formulation due to defects of our model in overestimating alpha particle production at low temperature.

Eq.(8) and Eq.(10) result in the transcendental equation for  $T$  as a function of plasma beta. It can be solved numerically, and the results are presented in figure 2, where the TAE

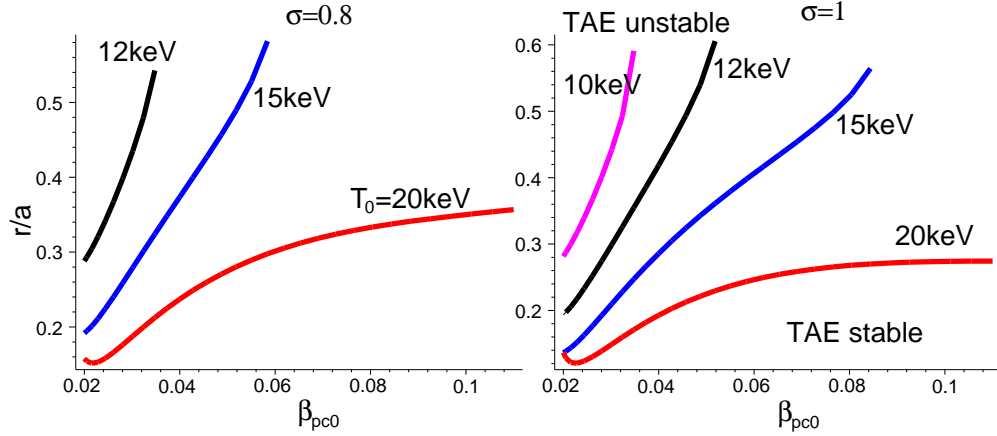


Figure 1: Critical  $r/a$  curves at which the instability is marginal for different temperatures of the plasma ions  $T_0 = 20, 15, 12, 10keV$ . On the left plotted are results for  $\sigma = 0.8$  and on the right for  $\sigma = 1$ .

ustable region lies above each curve. Here we fixed  $\eta = 1$ , i.e.  $r/a = 1/\sqrt{3} \simeq 0.58$ , which are the parameters we typically find for the most unstable surface. In plotting this and previous

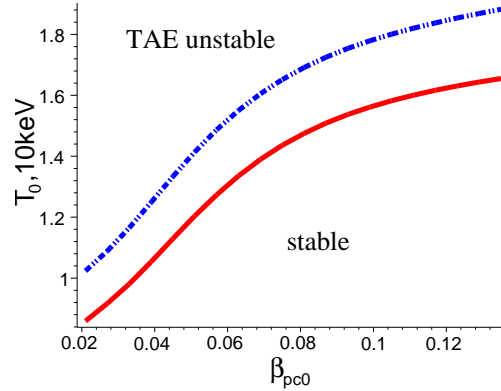


Figure 2: The stability diagram in the temperature - plasma beta plane for  $\eta = 1$  and depletion factors  $\sigma = 1$  (red solid curve),  $\sigma = 0.8$  (blue dash-dotted curve) is similar for three BP proposals being considered.

figures we fixed  $\epsilon = a/2R$ ,  $q = 1.5$ ,  $s = 1$ . As we mentioned for all machines, ITER, FIRE

and IGNITOR, the stability,  $T(\beta_{pc})$ , diagram in Fig.2 looks almost the same, so that shown is only the diagram with FIRE parameters.

### III. HINST MODELING OF TAE INSTABILITY

In this section we numerically explore the stability of TAE modes in the four different plasma experiments under the consideration. We use the TRANSP analyzing code [25] to obtain the appropriate profile parameters that is suitable for these tokamaks. In this study we employ the nonperturbative fully kinetic code HINST[7]. This code has recently been improved to account for finite orbit orbit effects and realistic geometry effects. In HINST use is made of the very efficient numerical equilibrium code ESC [26]. HINST shows agreement with NOVA growth rate calculations of core localized modes typically to within 20%. Below we compare HINST results with analytical dominant damping rates.

Figure 3 shows the cross sections of four devices being considered. The plasma parameters of these tokamaks are given in table II. In the estimates of the maximum toroidal mode

Tokamak	R,m	a,m	$B_0, T$	$n_{e0}, \frac{10^{14}}{cm^3}$	$T_{i0}, keV$	$\sigma$	$\beta_{\alpha 0}, \%$	$-R\nabla\beta_{\alpha}, \%$	$v_f/v_{A0}$	$v_A, 10^9 \frac{cm}{sec}$	$a/\rho_{\alpha 0}$	$n_{max}$
ITER-FEAT	6.2	2	5.3	1	19.3	0.78	0.7	5	1.8	0.72	39.1	10
FIRE	2.14	0.6	10	4.9	11.9	0.825	0.28	1.3	2.1	0.62	22.14	5
IGNITOR	1.32	0.48	13.1	9.4	9.9	0.91	0.2	0.8	2.21	0.59	23.2	5
JET-DT	2.92	0.94	3.82	0.45	23	0.795	0.4	2.3	1.66	0.78	13.25	4

Table II: Main plasma parameters for tokamaks under the consideration.

numbers we used Eq.(1) and assumed for all the machines  $r/aq^2 = 0.5$ . More detailed discussion of plasma parameters in BPs is published in Ref.[25]. We use the results of this paper to establish the plasma parameters profiles for the cases we study here. The profile variation of various parameters are shown in figures 4,5,6,7,8 as functions of the  $\sqrt{\Phi/\Phi_0}$ .

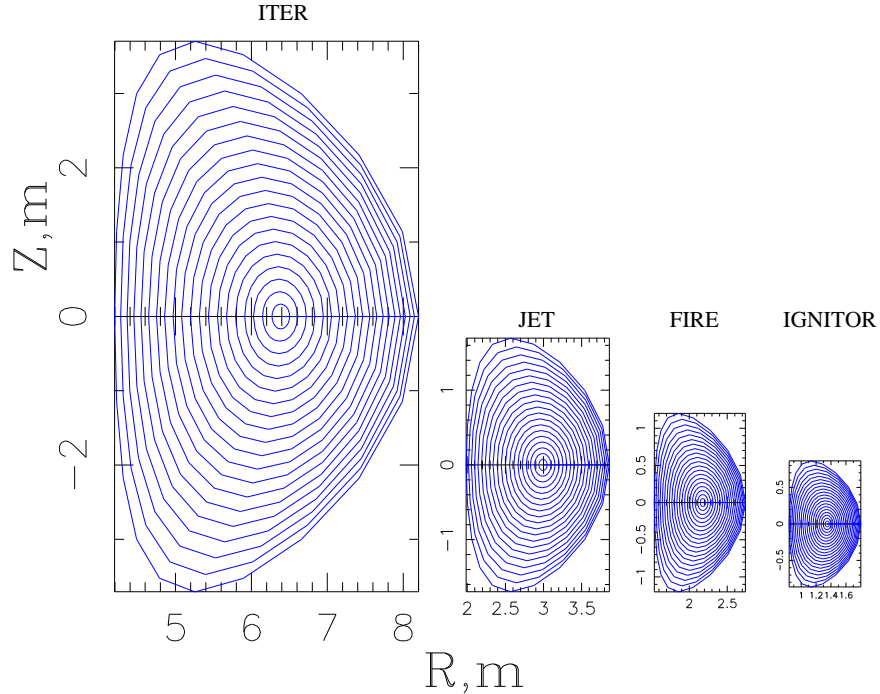


Figure 3: Plasma poloidal cross sections with magnetic surfaces of the four tokamaks under the investigation: FIRE, ITER, IGNITOR, and JET. Relative sizes of these machines are compared as shown.

Also shown is a “model”  $q$ -profile,  $q = 1 + 2.8 (\Phi/\Phi_0)^{3/2}$ , which will be used to establish the TAE stability effect on a common shear profile in all the machines considered here.

### A. Fusion Ignition Research Experiment (FIRE)

We first study the stability results for this machine in detail. Figure 9 shows the comparison of the analytical damping rate with TAE damping rate calculated by HINST code without fast particles. Here and below frequencies are normalized to the central Alfvén frequency  $\omega_{A0} = v_{A0}/q_0 R_0$ . The analytical damping rate includes ion Landau, Eq.(3), trapped electron collisional damping, Eq.(7), and radiative damping from Refs.[16, 21]. The dependences are given as functions of minor radius variable  $\sqrt{\Phi/\Phi_0}$ . The numerical damping

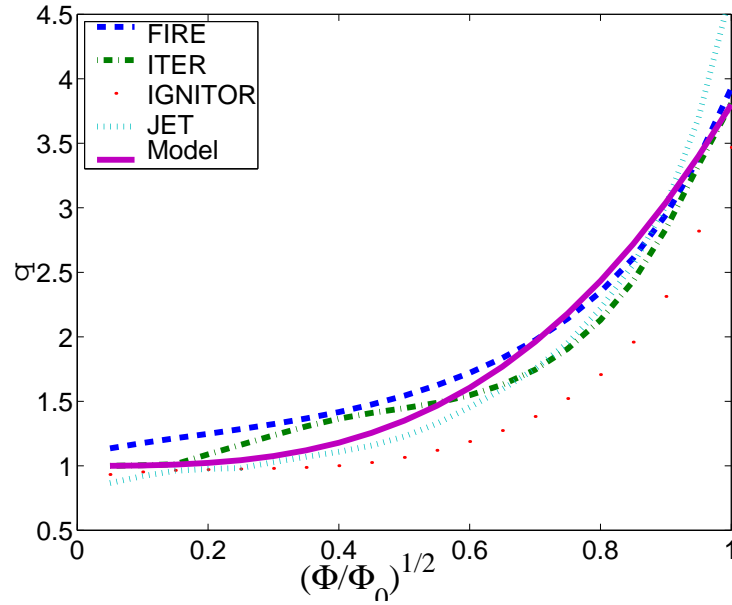


Figure 4: Safety factor profiles for four considered devices and the “model”  $q$ -profile used in HINST modeling.

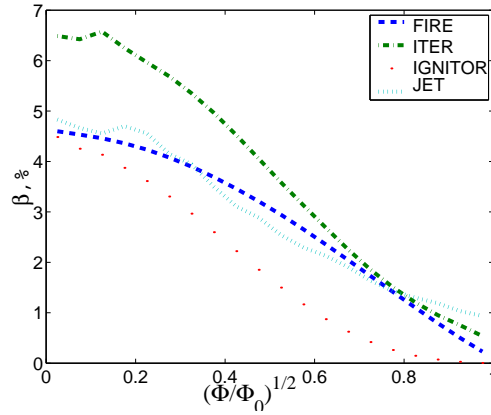


Figure 5: Total plasma beta profiles for four considered devices.

rates include radiative damping supported by thermal ion Landau and trapped electron collisional damping mechanisms. The results of the HINST code is in reasonable agreement with the analytical predictions within the radii  $0.35 < \sqrt{\Phi/\Phi_0} < 0.5$ , where the analytical

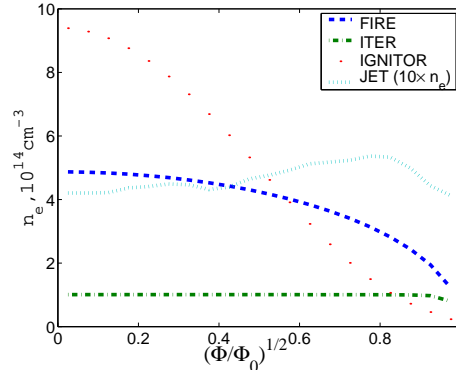


Figure 6: Electron density profiles for four considered devices.

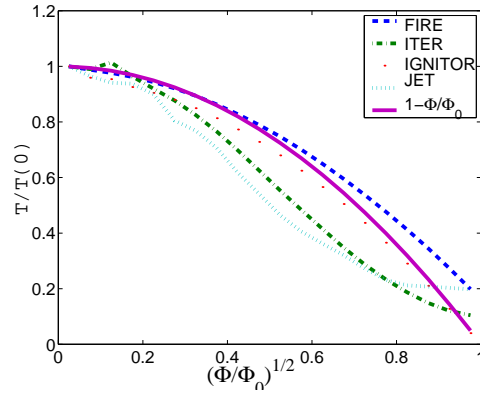


Figure 7: Normalized temperature profiles for four considered devices as compared with the parabolic profiles.

formulae can be applied. Closer to the edge,  $\sqrt{\Phi/\Phi_0} > 0.5$ , trapped electron collisional damping is the strongest damping mechanism, since the temperature decreases faster than the density, so that the collisional frequency increases with minor radius. In the typical instability region,  $\sqrt{\Phi/\Phi_0} \sim 0.5$ , ion Landau and trapped electron collisional damping are typically two competing mechanisms. Near the plasma center the frequency of core localized TAEs approaches lower continuum and the analytical formula for the radiative damping may not be valid. Note that the analytical ion Landau damping is within a factor of two from the HINST calculated damping (see also damping calculations for ITER below) and thus

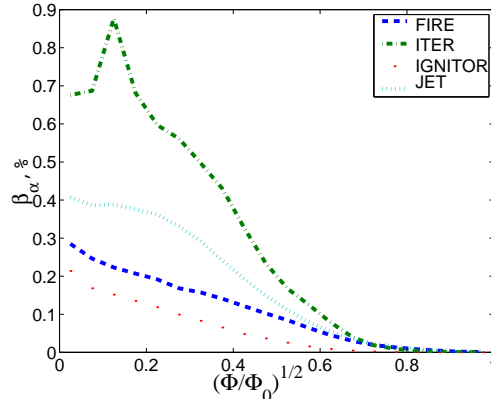


Figure 8: Alpha particle beta profile for four considered devices.

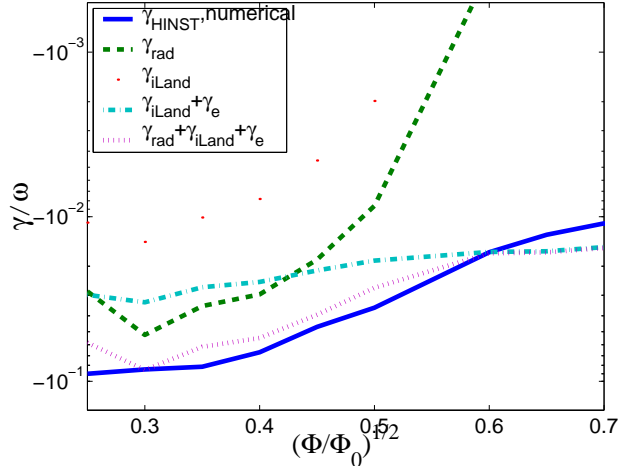


Figure 9: Comparison of numerical damping rates from HINST code with the analytical ones in FIRE for  $n = 10$  TAE.

reasonable approximation for the total damping.

For the TAE instability calculations we use TRANSP computed plasma core and  $\alpha$ -particle beta profiles shown in figures 5,8. The results from the HINST code for the nominal FIRE plasma are shown in figure 10 in the form of the eigenfrequency and the growth rate for TAEs as functions of  $\sqrt{\Phi/\Phi_0}$ , where TRANSP generated q-profile was used. Comparison of the instability using a model q-profile, and otherwise parameters from TRANSP, is shown

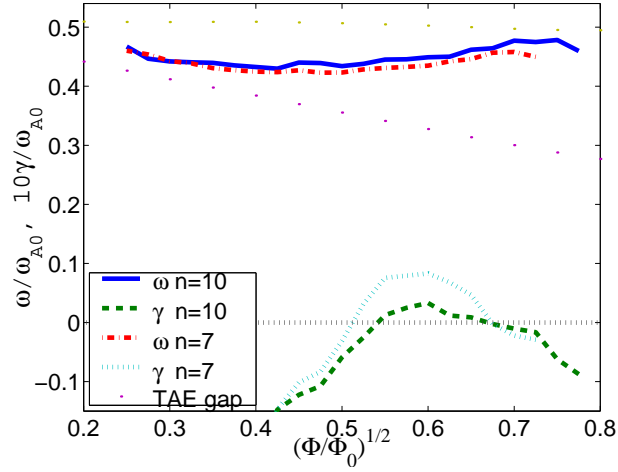


Figure 10: TAE eigenfrequency and growth rate as functions of minor radius variable  $\sqrt{\Phi/\Phi_0}$  in FIRE with TRANSP  $q$ -profile.

in figure 11 for FIRE  $n = 7$ . Figure 12 (FIRE curves) shows the eigenfrequency and the

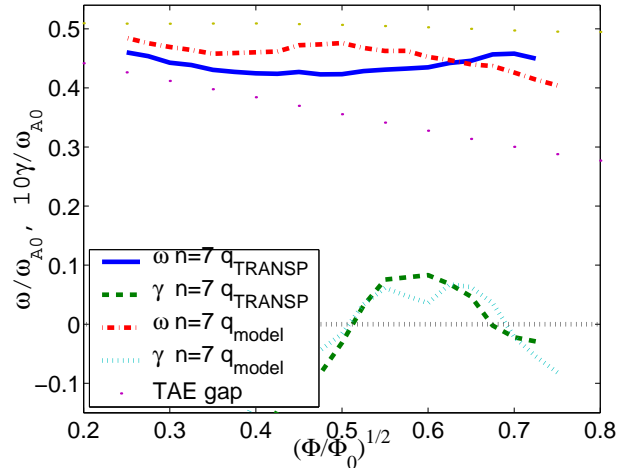


Figure 11: Comparison of TAE eigenfrequency and growth rates as functions of minor radius in FIRE for TRANSP and model  $q$ -profiles at fixed  $n = 7$ .

growth rate computed by HINST code for different toroidal mode numbers but taken on a surface with the strongest growth rate with model  $q$ -profile.

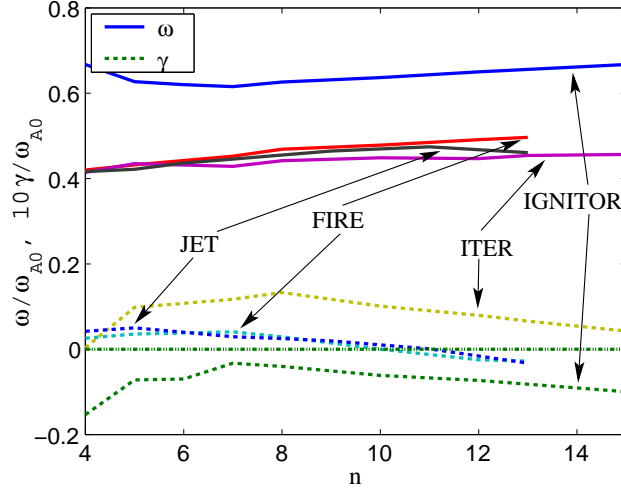


Figure 12: Eigenfrequency and growth rate of TAE vs. toroidal mode number as computed by HINST for four considered tokamaks with model  $q$ -profile and fusion  $\alpha$ -particle drive.

With TRANSP calculated central value of  $\beta_{\alpha 0} = 0.28\%$  TAE unstable region spans within  $0.5 < \sqrt{\Phi/\Phi_0} < 0.65$  and the growth rate sharply decreases outside. Since the solutions of TAEs typically have a global structure, the calculation for the stability requires taking an appropriate averaging over large portion of minor radius. Thus the final question of establishing a TAE critical beta requires a global calculation, such as performed in NOVAK whose results are described in the next section. Further, such an effect as stronger mode coupling through plasma shaping may introduce stronger continuum damping [27]. However, all global calculations are perturbative, which introduces another uncertainty. The perturbation theory presently used does not account for mode structure change induced by a strong drive and damping mechanisms that peak in different spatial regions. A more sophisticated perturbation theory may in turn result in a new instability arising from TAE localization around the region of strong drive.

The instability becomes stronger if at fixed plasma beta the temperature is increased and correspondingly the density is lowered. In the following example we keep the same temperature and density profiles as in the previous study but we changed only the central

values of following plasma parameters  $n_{e0} = 3.65 \times 10^{14} \text{ cm}^{-3}$ ,  $\beta_{pe0} = 5.6\%$ ,  $\beta_{\alpha 0} = 1.1\%$ ,  $T_{i0} = 21.4 \text{ keV}$  and used model  $q$ -profile. Results are shown in figure 13.

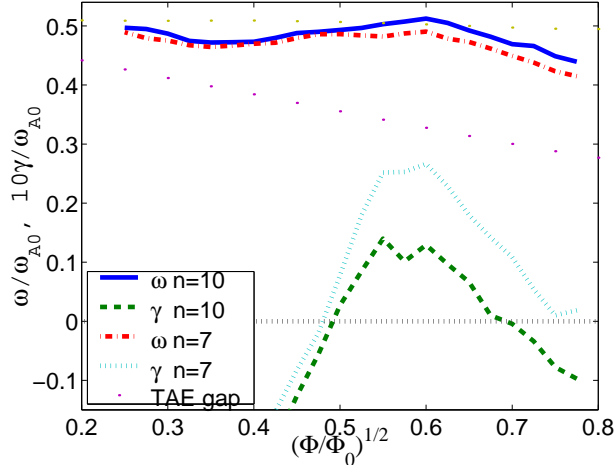


Figure 13: TAE eigenfrequency and growth rate as functions of minor radius in FIRE with model  $q$ -profile at higher plasma temperature.

## B. International Tokamak Experimental Reactor (ITER)

We performed similar TAE instability growth rate calculations for an ITER plasma. The numerical  $q$ -profile that emerges from TRANSP is not monotonic due to several factors, such as NBI and ICRH heating. We performed the calculations of the damping rates for the model  $q$ -profile shown in Fig.4. Figure 14 shows the comparison of TAE analytical damping rates (same as in FIRE study, Sec.III A) with damping rate by HINST code without  $\alpha$ -particles.

Figures 15 and 12 (ITER curves) represent the eigenfrequency and the growth rate of TAEs computed by HINST code as functions of  $\sqrt{\Phi/\Phi_0}$  and toroidal mode number  $n$ , respectively. As expected from our estimates in table II the maximum growth rate for ITER in the local calculations is shifted to higher  $n \simeq 9$ . In ITER the instability region is shifted towards smaller minor radii, which is primarily due to the lower damping that is present

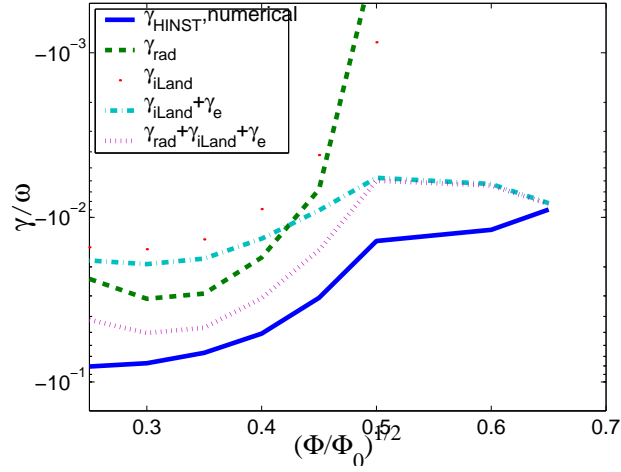


Figure 14: Comparison of numerical damping rates from HINST code with the analytical damping (same as in Sec.III A) rates in ITER for  $n = 10$  TAE.

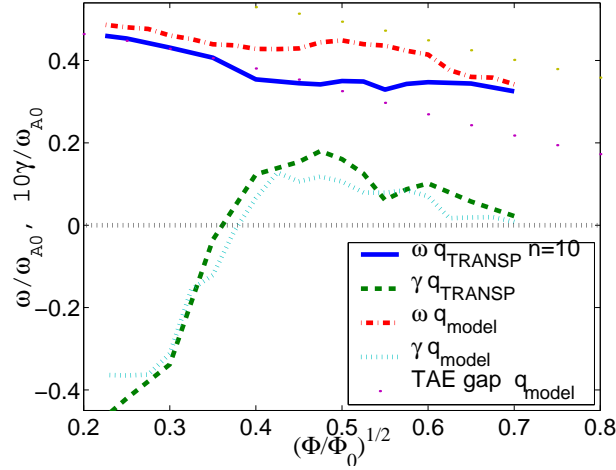


Figure 15: TAE eigenfrequency and growth rate as functions of the minor radius in ITER for model and TRANSP q-profiles.

$$\sqrt{\Phi/\Phi_0} \sim 0.5.$$

In ITER there are plans to use NBI heating (injected in the direction of plasma current). In order for beam particles to penetrate into the plasma, high energy beams have to be

used. At planned injection energy,  $\mathcal{E}_{b0} = 1MeV$ , beams contribute to the drive of TAEs for a wide range of  $n$ -values due to large driving,  $\omega_{*\alpha}$  term as a result of the strong anisotropy in velocity space of the beam ion distribution function. We will study the effect of beams in the next section, that reports the results of the NOVA calculations and show that  $1MeV$  beam ions contribute comparable terms to the instability as the alphas drive.

### C. IGNITOR

Figure 16 and 12 (IGNITOR curves) represent the eigenfrequency and the growth rate

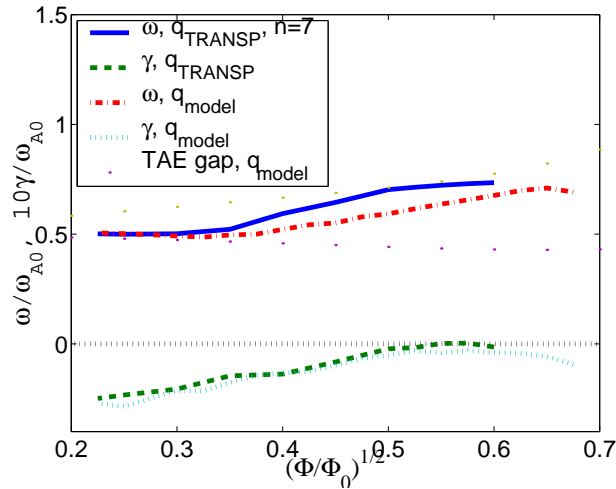


Figure 16: TAE eigenfrequency and growth rate as functions of minor radius in IGNITOR.

of TAEs computed by HINST code as functions of  $\sqrt{\Phi/\Phi_0}$  and toroidal mode number  $n$ , respectively. TAEs turn out to be robustly stable in IGNITOR, though sometimes close to the point of marginal stability. The stability is due to a low alpha particle beta that is a consequence of the lower plasma temperature than in the other proposed burning plasma proposals. This leads to a strong collisional damping on trapped electrons and a weaker drive. Global calculations are expected to give even stronger damping of TAEs.

### D. JET

As an attempt to experimentally validate our numerical predictions we analyze JET plasma. Figure 16 and 12 (JET curves) represent the eigenfrequency and the growth rate

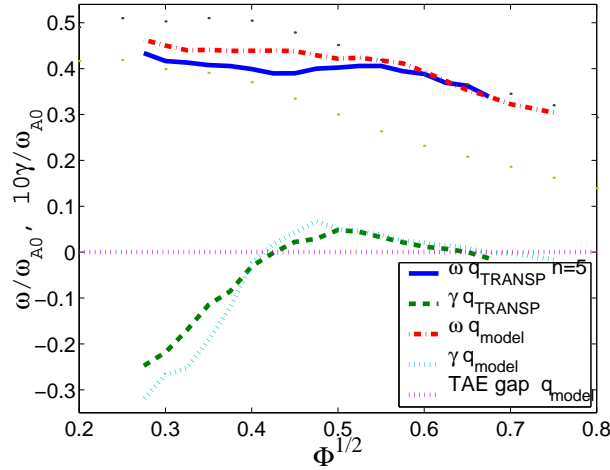


Figure 17: TAE eigenfrequency and growth rate as functions of minor radius in JET.

of TAEs computed by HINST code as functions of  $\sqrt{\Phi/\Phi_0}$  and toroidal mode number  $n$ , respectively. The maximum growth rate in JET, without beams, is rather low and is expected to be at  $n \simeq 6$ , which close to what was predicted in other studies [14, 28]. However with the NBI heating that was used, an additional strong stabilizing effect is present. We computed the TAE growth rate for an NBI beta  $\beta_b(0) = 0.6\%$  at an injection energy of deuterium  $\mathcal{E}_{b0} = 100keV$ . The calculations show that without fast particles the eigenfrequency at  $\sqrt{\Phi/\Phi_0} = 0.5$  and  $n = 5$ , is  $\omega/\omega_{A0} = 0.395 - i9 \times 10^{-4}$ . With alpha particles (no beams) we obtain  $\omega/\omega_{A0} = 0.402 + i4.8 \times 10^{-3}$ . With isotropic passing beam ions (no alphas and isotropic beams are used as at the moment the HINST code does not properly treat anisotropic beams) we obtain  $\omega/\omega_{A0} = 0.42 - i1.1 \times 10^{-2}$ . If we add the partial contributions to the growth rate from NBI ions and alphas we find that the TAEs should be stable primarily due to damping on beam ions. This conclusion is consistent with study in Refs.[14, 28]. As was expected in JET the number of unstable modes is less than for the burning plasma proposals  $\leq 7$ .

#### IV. NOVA MODELING OF TAE INSTABILITY

The advantage of using the HINST code is for its fast calculations, which allows us to focus study with more time consuming codes, such as NOVA, to the most unstable cases. NOVA modeling is based on a set of codes, which includes the ideal MHD computation of TAE eigenmodes [19] and the perturbative NOVAK postprocessing of the different driving and damping mechanisms such as fast particle pressure gradient drive with finite orbit width (FOW) and FLR effects, background ion and electron Landau damping, trapped electron collisional damping and radiative damping [19, 21, 22]. In the present study we apply NOVAK to ITER and FIRE with all of the plasma parameters provided by TRANSP. As we have shown IGNITOR and JET are stable in the local calculations, so that global studies are not expected to introduce any new destabilization to TAEs.

The following figures summarize this study for ITER, Fig.18, and FIRE, Fig..

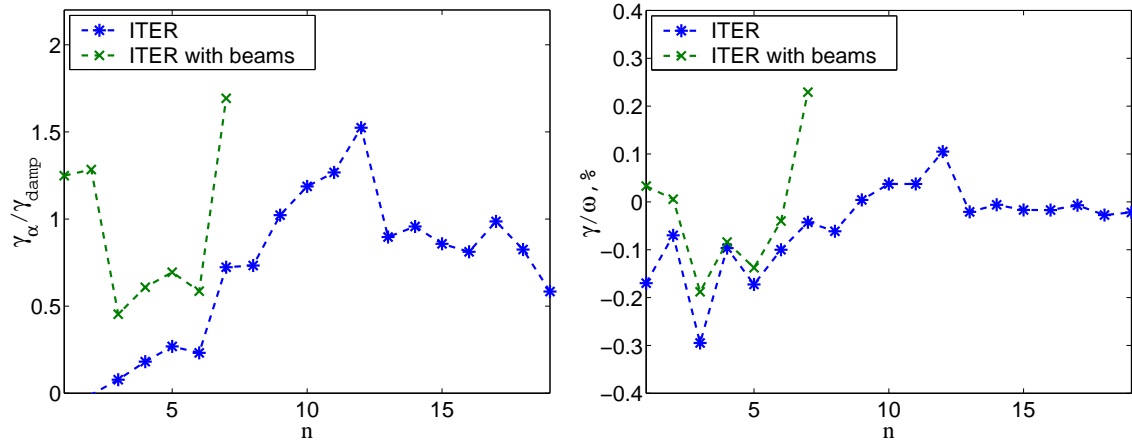


Figure 18: NOVAK calculations of AE growth rates for ITER. Shown are the maximum (among different modes for each  $n$ ) ratio of the alpha particle and  $\alpha$ -particle plus beam drive to the damping (left) and the maximum total growth rate of the modes with and without beams versus the mode toroidal number  $n$ .

In addition to TAE we analysed ellipticity (EAE) and triangularity (NAE) induced modes.

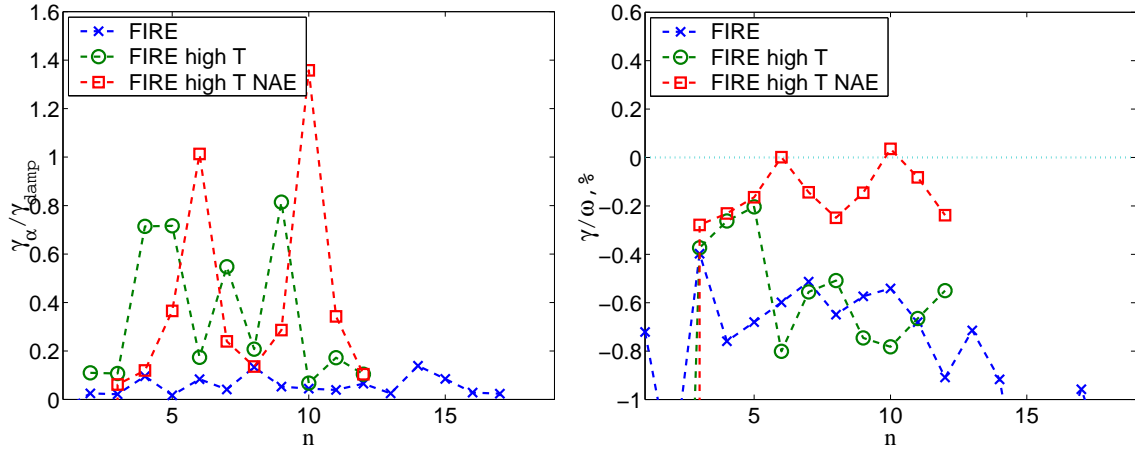


Figure 19: NOVAK calculations of TAE, EAE and NAE growth rates for FIRE. Shown are the maximum (among different modes for each  $n$ ) ratio of the alpha particle drive to the damping (left) and the total growth rate of the modes versus the mode toroidal number  $n$ .

ITER shows instability for these modes, which lies inside the gap. However these modes may interact with the continuum and may not be as unstable as the present predictions as the continuum interaction is not included in NOVA. As an example the mode structure of a TAE is shown in Fig. 20. We observe that it is localized well inside the gap, so that the mode may be expected to only weakly interact with the continuum.

FIRE study shows that all AEs are stable for the low temperature case outlined in Sec. III. However for the high temperature case TAEs and EAEs are marginally stable, while NAEs shows instability, which are localized near the core. Note that since the frequency of NAEs is a factor 3 larger than the frequency of the TAEs the ion Landau damping is significantly reduced due to exponentially small number of resonance thermal ions interacting with NAEs. The growth rate for NAEs is expected to be small. In previous experiments it was pointed out that NAEs have the lowest threshold of excitation when ICRH was applied [30]. There were no measurements of the effect of NAEs on fast particle confinement in those experiments.

To assess the effect from a neutral beam we take a distribution that is propagating nearly

parallel to the field lines, but with a small spread in pitch angle that is still larger than the mean pitch angle of the beam. One then has a slowing down distribution, multiplied by a weighting factor

$$f_\lambda(\lambda) = e^{-\lambda^2/\Delta_\lambda^2} \frac{4}{\Delta_\lambda \sqrt{\pi}},$$

where  $\lambda = v_\perp^2/Bv^2$ . With sufficiently small width,  $\Delta\lambda$ , the contribution of the anisotropy to the mode growth rate can be shown to be independent of  $\Delta\lambda$ . The Landau damping term due to fast beam ions is reduced by a factor of 3. It is important to note that beam ions may change the spectrum of unstable mode towards higher  $n$ -values. To reduce the beam ion contribution to the growth rate one can use beams with injection velocity smaller than the Alfvén velocity, so that the beam ions will not interact with the strongest resonance at the with Alfvén speed. The question remains whether such beams with energy  $\mathcal{E}_{b0} < 540keV$  can be deposited sufficiently deep into the plasma.

### A. Global versus local analysis in NOVAK

As we pointed out the global mode structure provides more stabilization. We performed a special study of this effect in ITER and FIRE. Analyzed eigenmodes of the TAE branch for FIRE,  $n = 7$  and ITER,  $n = 10$ , are shown in Fig. 20. Table summarises this study. For

	$\frac{\gamma_\alpha}{\omega}, \%$	$\frac{\gamma_b}{\omega}, \%$	$\frac{\gamma_{rad}}{\omega}, \%$	$\frac{\gamma_e}{\omega}, \%$	$\frac{\gamma_{eL}}{\omega}, \%$	$\frac{\gamma_{DLand}}{\omega}, \%$	$\frac{\gamma_{TLand}}{\omega}, \%$	$\frac{\gamma_\Sigma}{\omega}, \%$	$\left(\frac{\omega q_a}{\omega_{A0}}\right)^2$
FIRE, $n = 7$	2.26		-3.4	-26.5	-0.1	-0.9	-0.5	-29.	0.68
FIRE,pessimistic	8.9		-2.53	-0.9	-0.2	-2.45	-1.6	1.2	0.68
ITER, $n = 10$	0.29	0.36	-0.09	-0.27	-0.2	-0.1	-0.05	-0.06	1.21
ITER,pessimistic	1.28	0.88	-0.12	-0.14	-0.2	-0.43	-0.26	1.	1.21

Table III: The comparative results for global and “local” NOVA cases (when only two dominant harmonics are kept) for the growth and damping rate calculations for the FIRE high temperature case and ITER are presented here.

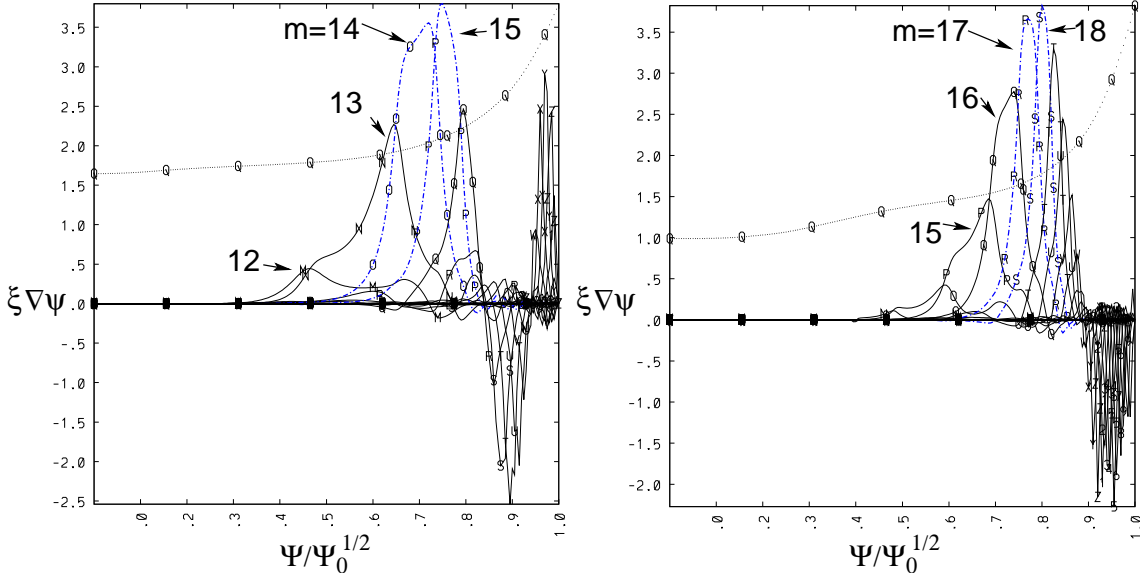


Figure 20: Eigenmode structure of TAEs in FIRE,  $n = 7$  (left) and ITER,  $n = 10$  (right). Shown as dash-dotted lines are harmonics used in “local” (more pessimistic for the stability) NOVA analysis, in which all other harmonics were excluded.

ITER and FIRE the local mode structure produces unstable modes. In FIRE, particularly for the high temperature case, the growth rate for the local mode is very strong up to  $\gamma/\omega \sim 10\%$ . Such a large value is perhaps indicative that the perturbative approach in NOVA calculations may not be justifiable. This issue needs to be addressed in future studies.

## V. CONCLUSIONS

Analyses of stability have been performed by three independent methods: analytical, numerical using the local kinetic nonperturbative HINST code, and numerical using the global code NOVA. These studies show that Alfvén modes should be robustly stable in IGNITOR, due to the lower fast particle beta and strong collisionality which leads to strong trapped electron collisional damping. Analytical and HINST calculations predict TAE instability in FIRE and ITER. Global perturbative code NOVA predicts TAEs in ITER to be slightly

unstable. However when instability is predicted there may be a significant stabilizing contribution from the continuum that has not been accounted for. We have noted that NBI at 1MeV strongly contributes to the drive with a growth rate comparable to the one due to fusion alphas. To make beam ions stabilizing one should decrease their energy below  $540keV$ , so that there will not be a direct resonance with TAEs. NBI with such injection energy need to satisfy the requirement of penetration into the core of the plasma.

For high temperature FIRE , NOVA predicts instability due to NAEs. At somewhat higher temperature,  $T_{i0} = 21.4keV$ , TAEs are marginally stable in FIRE. Our study raises the issue of whether the TAE perturbative analysis has been properly applied for ITER. We find strong local interactions that may break-up the large global extent of modes stabilized by large damping arising near the plasma edge. Since the modes occur at high  $n$ , where many eigenmodes have frequencies close to each other, it may be possible for instability to localize in the core when a more accurate is used.

- 
- [1] C. Z. Cheng, L. Chen, M. S. Chance, Ann Phys. (NY) **161**, 21 (1985).
  - [2] C. Z. Cheng and M. S. Chance, Phys. Fluids **29**, 3695 (1986).
  - [3] C. Z. Cheng, G. Y. Fu, and J. W. Van Dam, Princeton Plasma Physics Laboratory Report, PPPL-2585 (January, 1989), 14pp. *in Proceedings of the Joint Varrena-Lausanne Workshop on Theory of Fusion Plasmas*, Lausanne, Switzerland, Oct. 3-7, 1988, p. 259-270.
  - [4] G. Y. Fu and J. W. Van Dam, Phys. Fluids B **1**, 1949 (1989).
  - [5] K. L. Wong, Plasma Phys. Cont. Fusion **39** 2471 (1997).
  - [6] W. W. Heidbrink, Sadler, Nucl. Fusion **34**, 535 (1994).
  - [7] N. N. Gorelenkov, C. Z. Cheng, and W. M. Tang, Phys. Plasmas **5**, 3389 (1998).
  - [8] C. Z. Cheng, N. N. Gorelenkov, and C. T. Hsu, Nucl. Fusion **35**, 1639 (1995).
  - [9] L. Chen, Phys. Plasmas **1**, 1519 (1994).
  - [10] Briguglio et al., Phys. Plasmas Contr. Fusion **A279** 37 (1995).

- [11] R. A. Santoro and L. Chen, *Phys. Plasmas* **3**, 2349 (1996).
- [12] W. W. Heidbrink, E. J. Strait, M. S. Chu, and A. D. Turnbull, *Phys. Rev. Lett.* **71**, 855 (1993).
- [13] N. N. Gorelenkov and W. W. Heidbrink, *Nucl. Fusion* **42** (2002).
- [14] D. Borba, *et.al.*, *Nucl. Fusion* **40**, 775 (2000).
- [15] R. R. Mett and S. M. Mahajan, *Phys. Fluids B* **4**, 2885 (1992).
- [16] H. L. Berk, J. W. Van Dam, Z. Guo, and D. M. Lindberg, *Phys. Fluid B* **4**, 1806 (1992).
- [17] H. L. Berk, B. N. Breizman and H. Ye, *Phys. Letters A*, 475, (1992).
- [18] B. N. Breizman, S. E. Sharapov, *Plasma Phys. Cont. Fusion* **37** 1057 (1995).
- [19] C. Z. Cheng, *Phys. Fluid B* **3**, (1991).
- [20] H. L. Berk, R. R. Mett, and D. M. Lindberg, *Phys. Fluid B* **5**, 3969 (1993).
- [21] G. Y. Fu, C. Z. Cheng, R. Budny, *et.al.*, *Phys. Plasmas* **3**, 4036 (1996).
- [22] N. N. Gorelenkov, C. Z. Cheng, G. Y. Fu, *Phys. Plasmas* **7** 2802 (1999).
- [23] N. N. Gorelenkov, S. E. Sharapov, *Physica Scripta* **45** 163 (1992).
- [24] G. Y. Fu, C. Z. Cheng, *Phys. Fluids B* **4** 3722 (1992).
- [25] R. V. Budny, submitted to *Nucl. Fusion* **42**, (2002).
- [26] L. E. Zakharov and A. Pletzer, *Phys. Plasmas* **6** 4693 (1999).
- [27] A. Jaun, A. Fasoli, J. Vaclavik, L. Villard, *Nucl. Fusion* **40**, 1343 (2000).
- [28] S. Sharapov, *et.al.*, *Nucl. Fusion* **39**, 373 (1999).
- [29] *Plasma Physics and Controlled Nuclear Fusion Research* (International Atomic Energy Agency, Vienna, 1991), Vol. 3, p. 239.
- [30] G. J. Kramer, M. Saigusa, T. Ozeki, Y. Kusama, H. Kimura, T. Oikawa, K. Tobita, G. Y. Fu, and C. Z. Cheng, *Phys. Rev. Lett.* **80**, 2594 (1998).

## External Distribution

Plasma Research Laboratory, Australian National University, Australia  
Professor I.R. Jones, Flinders University, Australia  
Professor João Canalle, Instituto de Fisica DEQ/IF - UERJ, Brazil  
Mr. Gerson O. Ludwig, Instituto Nacional de Pesquisas, Brazil  
Dr. P.H. Sakanaka, Instituto Fisica, Brazil  
The Librarian, Culham Laboratory, England  
Library, R61, Rutherford Appleton Laboratory, England  
Mrs. S.A. Hutchinson, JET Library, England  
Professor M.N. Bussac, Ecole Polytechnique, France  
Librarian, Max-Planck-Institut für Plasmaphysik, Germany  
Jolan Moldvai, Reports Library, MTA KFKI-ATKI, Hungary  
Dr. P. Kaw, Institute for Plasma Research, India  
Ms. P.J. Pathak, Librarian, Insitute for Plasma Research, India  
Ms. Clelia De Palo, Associazione EURATOM-ENEA, Italy  
Dr. G. Grosso, Instituto di Fisica del Plasma, Italy  
Librarian, Naka Fusion Research Establishment, JAERI, Japan  
Library, Plasma Physics Laboratory, Kyoto University, Japan  
Research Information Center, National Institute for Fusion Science, Japan  
Dr. O. Mitarai, Kyushu Tokai University, Japan  
Library, Academia Sinica, Institute of Plasma Physics, People's Republic of China  
Shih-Tung Tsai, Institute of Physics, Chinese Academy of Sciences, People's Republic of China  
Dr. S. Mirnov, TRINITI, Troitsk, Russian Federation, Russia  
Dr. V.S. Strelkov, Kurchatov Institute, Russian Federation, Russia  
Professor Peter Lukac, Katedra Fyziky Plazmy MFF UK, Mlynska dolina F-2, Komenskeho  
Univerzita, SK-842 15 Bratislava, Slovakia  
Dr. G.S. Lee, Korea Basic Science Institute, South Korea  
Mr. Dennis Bruggink, Fusion Library, University of Wisconsin, USA  
Institute for Plasma Research, University of Maryland, USA  
Librarian, Fusion Energy Division, Oak Ridge National Laboratory, USA  
Librarian, Institute of Fusion Studies, University of Texas, USA  
Librarian, Magnetic Fusion Program, Lawrence Livermore National Laboratory, USA  
Library, General Atomics, USA  
Plasma Physics Group, Fusion Energy Research Program, University of California at San  
Diego, USA  
Plasma Physics Library, Columbia University, USA  
Alkesh Punjabi, Center for Fusion Research and Training, Hampton University, USA  
Dr. W.M. Stacey, Fusion Research Center, Georgia Institute of Technology, USA  
Dr. John Willis, U.S. Department of Energy, Office of Fusion Energy Sciences, USA  
Mr. Paul H. Wright, Indianapolis, Indiana, USA

The Princeton Plasma Physics Laboratory is operated  
by Princeton University under contract  
with the U.S. Department of Energy.

Information Services  
Princeton Plasma Physics Laboratory  
P.O. Box 451  
Princeton, NJ 08543

Phone: 609-243-2750  
Fax: 609-243-2751  
e-mail: [pppl\\_info@pppl.gov](mailto:pppl_info@pppl.gov)  
Internet Address: <http://www.pppl.gov>